https://doi.org/10.5194/wes-2025-230
Preprint. Discussion started: 13 November 2025

eawe european academy of wind energy
Open Access WIND ENERGY SCIENCE DISCUSSIONS

Multi-Scale Mapping of Sectional Stiffness Coupling in IEA 10MW,15 MW, and 22 MW Wind-Turbine Blades

Abhishek Sharma
VayuOra Energy, New Delhi, India
Correspondence: info@vayuoraenergy.com, abhikshar@gmail.com

Abstract
This study compares the spanwise stiffness and stiffness coupling characteristics of 10 MW, 15 MW, and 22 MW wind turbine blades using sectional 6×6 stiffness matrices extracted from NREL BeamDyn_blade input files. We define a normalized coupling coefficient and a root-mean-square (RMS) coupling score to map how axial–bending, shear–torsion, and bending–torsion interactions evolve along the blade span. With increasing scale, the 10 MW blade shows strong, localized coupling "hotspots" inboard, the 15 MW blade redistributes these interactions across mid-span, and the 22 MW blade exhibits weaker peak coupling but broader spatial influence extending toward the tip. This "smoothing with scale" indicates a design shift away from highly localized passive load alleviation and toward globally distributed aeroelastic tailoring for ultra-long (>130 m) blades. The method is fully reproducible from public OpenFAST model inputs. These findings provide crucial insights for the structurally-optimized and aeroelastically-stable design of next-generation megawatt-scale turbines.

1. Introduction

The drive to scale rotor diameters to capture more energy and reduce Levelized Cost of Energy (LCOE) is fundamentally challenged by the square-cube law. While power output scales with the *square* of the blade length, blade mass and critical loads often scale with the *cube*. This disparity means that simply geometrically scaling existing designs is structurally inefficient and can lead to excessive mass. More critically, it results in significantly more flexible blades, where complex structural couplings—such as bend-twist effects—become pronounced and can compromise aeroelastic stability through phenomena like flutter.

Current comparisons of reference turbines often focus on overall performance, lacking a detailed, spanwise quantification of the complex cross-sectional stiffness that drives aeroelastic response. This paper addresses this gap by performing a comparative analysis of the NREL 10 MW, IEA 15 MW, and 22 MW blade. The objective is to critically quantify the evolution of spanwise stiffness coupling by analyzing the full suite of sectional stiffness matrices used as input for the high-fidelity beam solver, BeamDyn. The findings aim to provide crucial insights for achieving structurally efficient and aeroelastically stable designs for the next generation of ultra-large wind turbines.

2. Literature Review

https://doi.org/10.5194/wes-2025-230
Preprint. Discussion started: 13 November 2025

Several earlier studies have provided valuable insights into wind-turbine blade coupling and scaling, establishing a foundation for the present work.

At the material and sub-structural level, Fedorov and Berggreen, 2014 explored the potential of bend–twist coupling (BTC) in wind turbine blades using both numerical and experimental approaches. By reducing the stiffness matrix to a 2×2 compliance model, they quantified coupling magnitudes up to 0.4 for carbon-fiber composite laminates, validating results against BECAS simulations and digital image correlation (DIC) measurements. However, their work was limited to small-scale prototypes, with no assessment of coupling distribution along the blade span or scaling to multi-megawatt rotors.

Building upon this, Chen et al., 2021 conducted a sensitivity analysis of the 6×6 sectional stiffness matrix of the NREL 5 MW reference blade, evaluating how individual stiffness components influence aeroelastic response under steady and turbulent inflow. They found that diagonal stiffnesses (EA, EI_flp, GJ) primarily govern root bending and tip displacement, while coupling terms K_{16} and K_{56} (axial–flap and flap–torsion) strongly affect dynamic stability and fatigue loads. This work highlighted the structural importance of coupling but remained confined to a single blade scale and parametric stiffness variation, without examining how such couplings evolve with geometric upscaling.

The NREL rotor-scaling study by Jonkman, 2021 established the foundational geometric laws that govern large-rotor scaling, confirming that bending stiffness scales as $EI \propto R^4$ and mass per unit length as $\mu \propto R^2$. While these relations underpin current megawatt-class turbine design, they treat stiffness in aggregate form — omitting distributed or directional effects and ignoring coupling between degrees of freedom.

Complementary findings from Larwood et al., 2014 on swept-blade design further revealed how geometric modifications influence stiffness and stability. Their parametric study across 1.5 MW, 3 MW, and 5 MW rotors demonstrated that backward sweep reduces flapwise fatigue loads and improves energy capture by up to 5 %, but simultaneously shifts the elastic axis away from the mass center. This increases torsional compliance and coupling sensitivity, especially near the flutter boundary for larger blades.
Larwood and colleagues emphasized that, beyond 5 MW, aeroelastic instabilities emerge from insufficient torsional stiffness (GJ) and geometric coupling — foreshadowing the challenges now observed in ultra-long (> 100 m) blades.

More recent advances by Zhuang and Yuan ,2021 examined the aerodynamic and structural consequences of bend–twist coupling in the IEA 15 MW reference blade using high-fidelity aeroelastic simulations. Yet, this and other works focus primarily on local coupling within a fixed rotor, without tracing how distributed stiffness interactions evolve with blade size.

While prior studies have laid the foundation for understanding coupling at material, geometric, and aeroelastic levels, a systematic, multi-scale mapping of the full 6×6 stiffness matrix across multiple turbine sizes remains unexplored.
Most previous analyses:

https://doi.org/10.5194/wes-2025-230
Preprint. Discussion started: 13 November 2025

- Are limited to a single turbine scale (≤ 5 MW or 15 MW).
- Rely on simplified coupling formulations (2×2 submatrices).

Examine coupling qualitatively through sweep or fiber bias rather than *quantitative stiffness data*.

This study addresses that gap through a comparative stiffness-matrix analysis of the IEA 10 MW, IEA 15 MW, and 22 MW blades. However, no prior work has published a spanwise, matrix-level comparison of stiffness coupling terms across multiple utility-scale reference turbines (10MW,15MW,22 MW) using directly parsed BeamDyn_blade inputs. This paper fills that gap.

3. Model and Geometry Description

We analyse three blades, the model parameters are shown in Table 1:

- IEA 10 MW Wind turbine
- IEA 15 MW Wind turbine
- IEA 22 MW Wind turbine

The data for the IEA 10 MW, 15 MW, and 22MW reference turbines, we used published primary input files (such as *.dat files for BeamDyn_blade, AeroDyn15_blade, ElastoDyn_blade) that define chord, twist, pitch-axis, structural twist, and the full 6×6 sectional stiffness matrix K(s) at each blade station. The files are available at the NREL official OpenFAST model repositories.

Table 1: Model Parameters

Parameter	Wind Turbines		
	10 MW	15 MW	22 MW
Rotor Diameter (m)	198	240	284
Blade Length (m)	96.75	117	137.8

Figure 1 :10 MW blade profile, Chord rises rapidly from the root to a broad maximum at η: 0.15–0.25, then tapers nearly linearly to the tip. Twist decreases steeply over the first 25 m and then relaxes toward the tip, ending slightly negative.

Figure 2 : 15 MW blade profile, where the peak chord occurs at a similar relative span, but the taper is smoother and extends over a longer physical distance. The twist schedule is steeper inboard than for the 10 MW case and remains more negative outboard.

Figure 3 : 22 MW blade profile, where both chord and twist distributions are further “flattened”: the transition from the inboard peak chord to the outboard taper is more gradual, and the twist evolves smoothly across the span.

https://doi.org/10.5194/wes-2025-230
Preprint. Discussion started: 13 November 2025

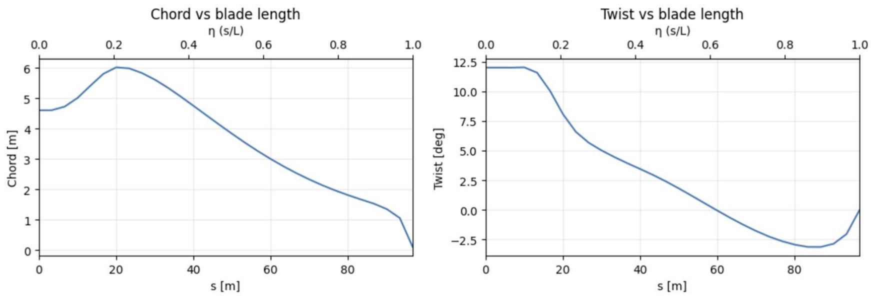

Figure 1. Chord and twist distribution along the span of the 10 MW blade.

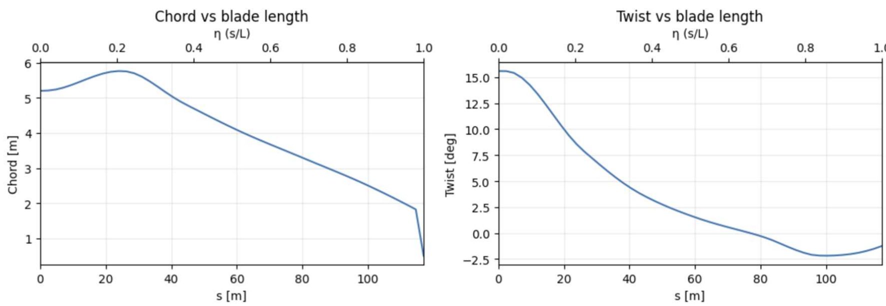

Figure 2. Chord and twist distribution along the span of the 15 MW blade.

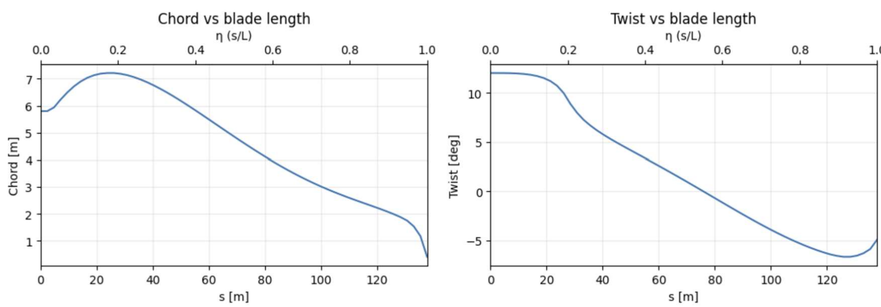

Figure 3. Chord and twist distribution along the span of the 22 MW blade.

The6×6 stiffness matrix Ki,j represents local sectional stiffness properties extracted from BeamDyn_blade input files as kept in official OpenFast model repositories. Each section's stiffness matrix results from composite lay-ups defined by varying fiber orientation angles

https://doi.org/10.5194/wes-2025-230
Preprint. Discussion started: 13 November 2025

and thicknesses across the chord. The degrees of freedom and corresponding stiffness terms are as follows.

Table 2: Stiffness Matrix

Matrix Term	Coupled DOFs	Physical Interpretation	Type
K_{11}	Flapwise shear (y)	Flapwise shear stiffness (K_shr,flp)	Diagonal
K_{22}	Edgewise shear (z)	Edgewise shear stiffness (K_shr,edg)	Diagonal
K_{33}	Axial extension (x)	Axial stiffness (EA)	Diagonal
K_{44}	Edgewise bending (My)	Edgewise bending stiffness (EI_edg)	Diagonal
K_{55}	Flapwise bending (Mz)	Flapwise bending stiffness (EI_flp)	Diagonal
K_{66}	Torsion (x)	Torsional stiffness (GJ)	Diagonal
K_{12}, K_{21}	Flapwise ↔ Edgewise shear	Shear–shear coupling	Off-diagonal
K_{13}, K_{23}	Shear ↔ Axial	Tension–shear coupling	Off-diagonal
K_{14}, K_{15}, K_{24}, K_{25}	Shear ↔ Bending	Bending–shear coupling	Off-diagonal
K_{16}, K_{26}, K_{36}	Shear/Axial ↔ Torsion	Shear/tension–torsion coupling	Off-diagonal
K_{34}, K_{35}	Axial ↔ Bending	Tension–bending coupling	Off-diagonal
K_{46}, K_{56}	Bending ↔ Torsion	Bend–twist coupling	Off-diagonal

4. Methodology

This parametric study employs a systematic methodology for extracting, processing, and analyzing spanwise stiffness properties from the NREL/IEA 10 MW, 15 MW, and 22 MW reference turbine. The core data, comprising the full 6×6 sectional stiffness matrices, was obtained from the respective BeamDyn_blade input files (.dat).

A custom Python script, developed in a Google Colab environment utilizing NumPy and Pandas, was created to automate the data extraction. The script parses each input file, identifies the DISTRIBUTED_PROPERTIES section, and stores the sequence of 6×6 stiffness matrices K(s) for each blade station as structured arrays.

To enable a scale-invariant comparison of coupling effects and the evolution of stiffness, the following normalization procedures were applied:

a) Normalized Coupling Coefficient: $\hat{K}_{ij} = K_{ij}/\sqrt{K_{ii}K_{jj}}$. This non-dimensional metric quantifies the strength of interaction between different degrees of freedom (e.g., axial-edgewise, flapwise-torsional), with values ranging from -1 to 1.

b) Normalized Span Coordinate: $\eta = s/L$. This defines the dimensionless blade span, allowing for direct comparison of structural trends across different blade lengths.

https://doi.org/10.5194/wes-2025-230
Preprint. Discussion started: 13 November 2025

To provide a single, comprehensive indicator of the overall structural coupling intensity along the span, a Root Mean Square (RMS) coupling score. It is indicator of how strongly the blade section is structurally coupled, we define a root-mean-square (RMS) coupling score.

a) For each blade station, we computed an overall coupling intensity score by collapsing the full 6×6 sectional stiffness matrix into a single scalar.
b) The normalized sectional stiffness matrix K(i,j), where the diagonal terms represent the principal bending, torsional, and axial stiffnesses, and the off-diagonal terms represent the various coupling pathways (e.g. flap–torsion, edge–torsion, flap–edge).

c) At each spanwise locations s, we set all diagonal terms of K(i,j) to NaN and retained only the off-diagonal terms. We then computed the root-mean-square (RMS) magnitude of those off-diagonal terms:

$$K_{\text{RMS}}(s) \;=\; \sqrt{\text{mean}\ (K_{ij}(s)^2)_{i\neq j}}.$$

The resulting normalized coupling coefficients and stiffness profiles were visualized using Matplotlib, employing both 2D line plots and heat maps to elucidate spanwise trends. This facilitated a direct comparative analysis of key coupling interactions, such as EA–EI_edg and GJ–EI_flap, across the 10 MW, 15 MW, and 22 MW configurations.

5. Results and Discussion

5.1 Coupling Characteristics – 10 MW Wind Turbine Blade

The 10 MW blade exhibits pronounced coupling effects, primarily between edgewise bending (EI_edg) and axial stiffness (EA), and between flapwise shear (K_shr,flp) and torsion (GJ). Heat Map plotted as shown in Figure 4 reveals a strong outof-phase (negative) coupling band around mid-span (η: 0.3–0.7), where the EA ↔ EI_edg interaction dominates. In contrast, a positive coupling is observed for EA ↔ EI_flp, suggesting in-phase deformation tendencies where axial extension may be supported by flapwise bending.

Figure 5 confirms these trends, showing the EI_edg ↔ EA coupling growing towards mid-span before decaying toward the tip, while K_shr,flp ↔ GJ remains moderate (0.6 at η: 0.4). Figure 7 shows the RMS coupling strength rising sharply from the root to η: 0.25, plateauing near 0.2, and then decaying toward the tip. This indicates that the most significant structural interactions are concentrated in the inboard region.These observed features are a direct result of the blade's structural design. The strong couplings in the mid-span and inboard regions are characteristic of the thick composite laminates and significant chord-twist gradients in these areas as shown in Figure 6. This pronounced bend-twist coupling, a hallmark of modern composite blades, is intentionally designed for passive load alleviation.

https://doi.org/10.5194/wes-2025-230
Preprint. Discussion started: 13 November 2025

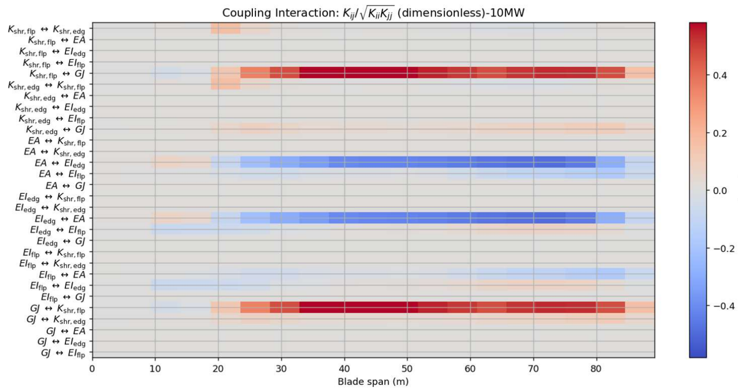

Figure 4. Normalized stiffness coupling matrix for the 10 MW blade.

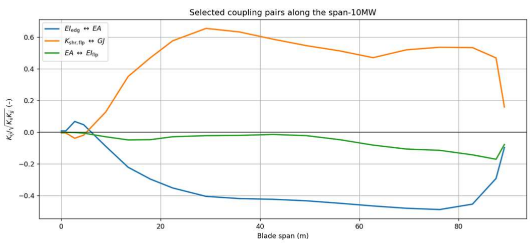

Figure 5. Selected coupling terms (e.g. EA↔EI_edg, shear↔torsion) for the 10 MW blade.

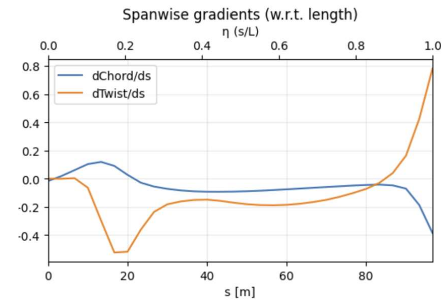

Figure 6. Chord and twist gradients (dChord/ds, dTwist/ds) for the 10 MW.

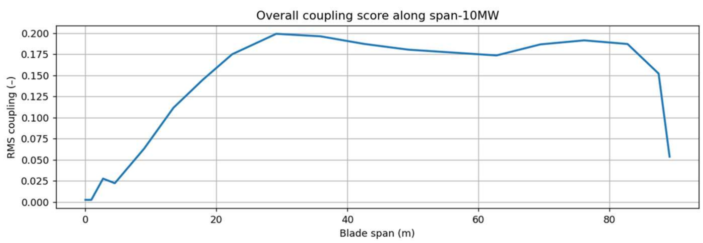

Figure 7: Overall Coupling Score for 10MW Wind Turbine.

https://doi.org/10.5194/wes-2025-230
Preprint. Discussion started: 13 November 2025

eawe european academy of wind energy
Open Access WIND ENERGY SCIENCE DISCUSSIONS

5.2 Coupling Characteristics – 15 MW Wind Turbine Blade

Scaling to the 15 MW blade leads to a noticeable redistribution of coupling effects along the span. Heat Map plotted as shown in Figure 8 reveals a strong in-phase (positive) coupling band around mid-span (η: 0.3–0.8), where the EA ↔ EI_edg interaction dominates. In contrast, a positive coupling is observed for EA ↔ EI_flp, suggesting out of -phase deformation tendencies where axial extension may be opposed by flapwise bending. Meanwhile, the K_shr,flp ↔ GJ coupling is visible but weaker than in the 10 MW blade, consistent with a altered shear-to-torsional stiffness ratio.

Figure 9 indicates that EI_edg ↔ EA peaks around η: 0.3–0.4, while Figure 10 shows an overall RMS coupling of 0.1 at mid-span, tapering toward the tip.

This redistribution signifies a maturation in structural tailoring. The shift suggests that for the 15 MW scale, designers have successfully spread the coupling effects to achieve load alleviation benefits.

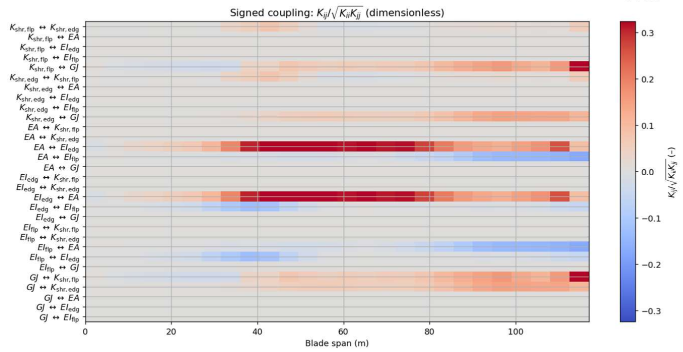

Figure 8. Normalized stiffness coupling matrix for the 15 MW blade.

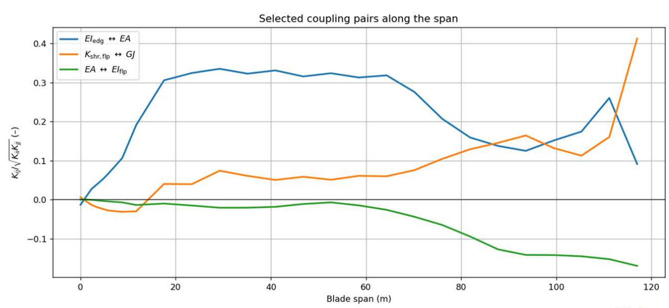

Figure 9. Selected coupling terms for the 15 MW blade.

https://doi.org/10.5194/wes-2025-230
Preprint. Discussion started: 13 November 2025

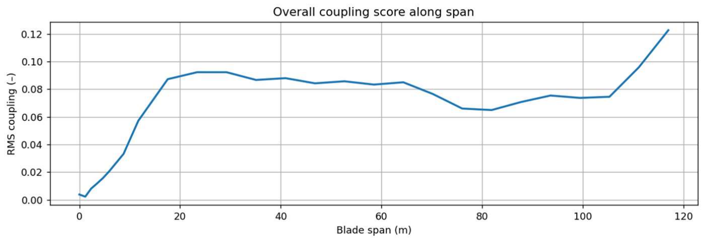

Figure 10. RMS coupling score for the 15 MW blade.

5.3 Coupling Characteristics – 22 MW Wind Turbine Blade

In the 22 MW blade, a key trend emerges: while peak coupling magnitudes reduce slightly, their spatial influence broadens significantly. Figure. 11 reveals smoother transitions along the span, with moderate coupling (0.15 – 0.25) for EA ↔ EI_edg and K_shr,flp ↔ GJ extending nearly to the tip (η: 0.9).

Figure. 12 shows a flatter mid-span behavior for EI_edg ↔ EA, with peaks shifted towards the root and tip. Consequently, Figure. 13 depicts a lower and more broadly distributed RMS coupling (0.07 – 0.09). This observed "smoothing" of the coupling landscape is a critical evolutionary step for ultra-long blades. It implies that to maintain aeroelastic stability and control load paths at this scale, structural anisotropy must be more carefully balanced. This is likely achieved through advanced design strategies, such as the use of carbon fiber spar caps for global stiffness control and refined twist tailoring. The shift from localized, high-intensity couplings to distributed, moderate coupling indicates a design optimized.

https://doi.org/10.5194/wes-2025-230
Preprint. Discussion started: 13 November 2025

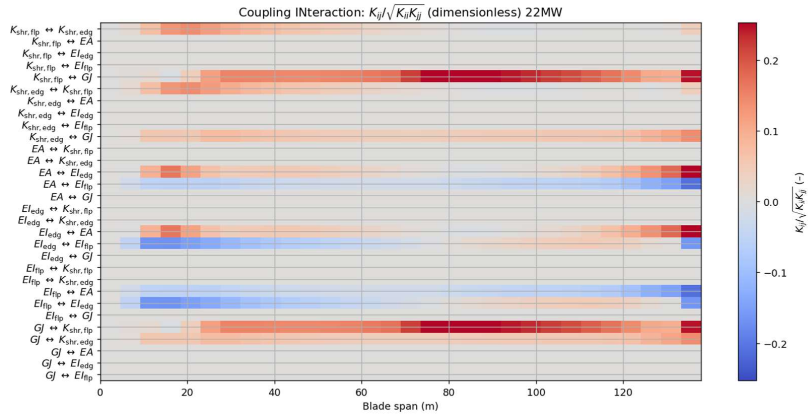

Figure 11. Normalized stiffness coupling matrix for the 22 MW blade.

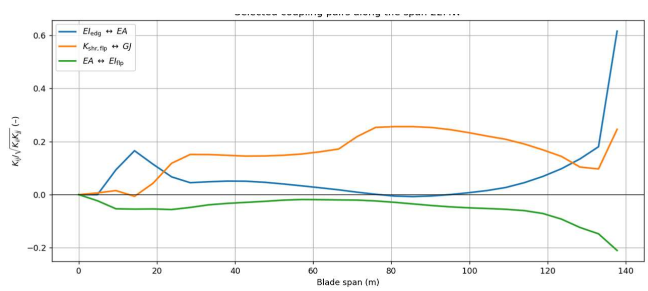

Figure 12. Selected coupling terms for the 22 MW blade.

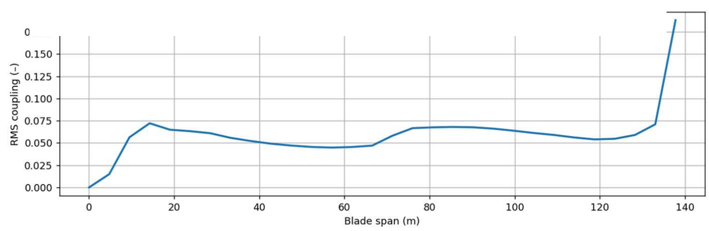

Figure 13. RMS coupling score for the 22 MW blade.

5.4 Cross-Scale Interpretation

The comparative analysis across the 10 MW, 15 MW, and 22 MW blades reveals a clear evolutionary design trend, summarized in Table 4.

https://doi.org/10.5194/wes-2025-230
Preprint. Discussion started: 13 November 2025

Table 4. Evolution of stiffness coupling characteristics across turbine scales

Blade	Dominant Coupling	Peak K̂_ij	RMS Coupling	Key Design Insight
10 MW	K_shr,flp ↔ GJ and EA ↔ EI_edg	≈ 0.5	0.2	Strong, localized mid-span interactions.
15 MW	EA ↔ EI_edg > EA ↔ EI_flp	≈ 0.35	0.1	Redistributed coupling; improved structural tailoring.
22 MW	EA ↔ EI_edg ~ K_shr,flp ↔ GJ	≈ 0.25	0.07	Distributed, smoothed coupling for stability.

The progression from 10 MW to 22 MW illustrates a deliberate design evolution away from high, localized coupling "hotspots" and towards a more homogenized distribution of structural interactions. This trend reflects an engineering priority for larger blades: managing aeroelastic stability and load control across a more flexible structure becomes paramount. The reduction in peak coupling values, coupled with their broader distribution, suggests that for blades beyond 130 meters, potentially at the expense of the strong, localized passive load alleviation effects seen in smaller designs.

6. Conclusions

This study has systematically quantified the evolution of spanwise stiffness coupling in wind turbine blades across three scales: the NREL 10 MW, IEA 15 MW, and 22 MW Wind Turbines. By extracting and analyzing the full 6×6 sectional stiffness matrices, we have moved beyond simplified models to provide a comprehensive, matrix-level comparison.

The key finding is a clear evolutionary trend in coupling characteristics with increasing blade scale. The 10 MW blade exhibits strong, localized coupling, particularly between flapwise shear and torsion (K_shr,flp ↔ GJ) and axial and edgewise bending (EA ↔ EI_edg), concentrated in the mid-span region. As scale increases to 15 MW, these coupling effects redistribute along the span, with peak magnitudes decreasing—a signature of improved structural tailoring. For the 22 MW blade, this trend culminates in a further reduction of peak coupling coefficients but a significant broadening of their spatial influence, resulting in a more homogenized stiffness landscape.

These observations lead to two fundamental insights for the design of 20 MW+ turbines:

1. The design priority shifts from leveraging strong, localized passive load alleviation to the smoothed coupling distribution in the 22 MW blade reflects a necessary adaptation to maintain controllability and prevent flutter in ultra-long, flexible blades.

https://doi.org/10.5194/wes-2025-230
Preprint. Discussion started: 13 November 2025

2. Geometric and structural scaling is inherently non-linear regarding stiffness interactions, the internal coupling anisotropy does not scale uniformly, requiring deliberate design compensation, likely through advanced material layups and twist tailoring.

These findings provide directly usable metrics for early-stage design screening of blades beyond 20 MW: the spanwise bandwidth of coupling is as important as the peak magnitude.

7.Data availability

The sectional stiffness matrices and blade-property distributions (chord, twist, pitch axis, structural twist) used for the 10-, 15-, and 22-MW reference turbines (OpenFAST /AeroDyn /ElastoDyn/BeamDyn input files) are available in our GitHub repository [IEA-10.0-198-RWT/openfast at master · IEAWindSystems/IEA-10.0-198-RWT, IEAWindSystems/IEA-15-240-RWT: 15MW reference wind turbine repository developed in conjunction with IEA Wind, IEAWindSystems/IEA-22-280-RWT: Repository for the IEA 22-MW offshore reference wind turbine developed by the IEA Wind Task 55 REFWIND].

8.Code availability

The Python scripts used to parse the OpenFAST blade definition files, compute gradients, construct the normalized coupling coefficient, RMS coupling score, and generate all figures.

9.Author contributions

Abhishek Sharma conceived the study, developed the analysis scripts, performed the data extraction, generated the figures, interpreted the results, and wrote the manuscript.

10.Competing interests

The author is the founder of VayuOra Energy, New Delhi, India. The authors declare that they have no conflict of interest.

11.Acknowledgements

The author thanks the developers and maintainers of the publicly available IEA / NREL reference turbine models that enable open analysis. The author also used an AI language model (ChatGPT, OpenAI) to assist with debugging Python scripts for extracting sectional stiffness data and refine the clarity and readability of the manuscript. All engineering interpretations, and conclusions are the author's own.

12. References

1. Chen, C., Wang, T., & Wang, L. (2021). *Sensitivity study of the influence of blade sectional stiffness parameters on the aeroelastic response of wind turbines.* Frontiers in Energy Research, 9, 707082.

https://doi.org/10.5194/wes-2025-230
Preprint. Discussion started: 13 November 2025

eawe european academy of wind energy
Open Access WIND ENERGY SCIENCE DISCUSSIONS

2. Fedorov, V., & Berggreen, C. (2014). *Bend–twist coupling potential of wind turbine blades.* Composite Structures, 116, 12–21.
3. Larwood, S., Zuteck, M., Snowberg, D., & van Dam, C. (2014). *Design studies of swept wind turbine blades.* Renewable Energy, 71, 563–571.
4. Zhuang, X., & Yuan, Y. (2024). *The impact of bend–twist coupling on structural characteristics and flutter limit of ultra-long flexible blades.* Energies, 17(8), 3450.
5. Jonkman, J. (2021). *On the scaling of wind turbine rotors.* Wind Energy Science, 6, 1165–1184.
6. Technical report by IEA Wind TCP Task 37, Definition of the IEA Wind 15-Megawatt Offshore Reference Wind Turbine
7. Technical report by IEA Wind TCP Task 55, Definition of the IEA Wind 22-Megawatt Offshore Reference Wind Turbine